Asian Transport Studies, Volume 2, Issue 1 (2012), 93-108

Optimization of Housing Allocation and Transport Emissions Using Continuum Modeling Approach

Jun YIN [a], Sze Chun WONG [b], Nang Ngai SZE [c]

[a,b,c] *Department of Civil Engineering, The University of Hong Kong, Pokfulam Road, Hong Kong*
[a] *E-mail: yinjun2005@gmail.com*
[b] *E-mail: hhecwsc@hku.hk*
[c] *E-mail: nnsze@graduate.hku.hk*

Abstract: The impact of vehicle emissions on the global climate has drawn increasing concern in the past few decades. Patterns of housing development determine travel behaviors, thus affecting transport-related greenhouse gas emissions. Here, a bi-level model is established to describe the relationships among housing allocation, traffic volume, and CO_2 emissions using a continuum modeling approach. The user-equilibrium condition is achieved in the lower-level, and the minimum CO_2 emissions are obtained by optimization the housing allocation in the upper-level. A hypothetical city is considered with one central business district (CBD) and a road network that is densely distributed outside of the CBD. Several commuter classes with different values of time are considered. The finite element method, the Newton-Raphson algorithm, and the convex combination approach are applied to solve the constrained optimization problem established in the bi-level model. A numerical example is given to demonstrate the effectiveness of the method.

Key words*: Continuum modeling, Transport emission, Housing allocation pattern*

1. INTRODUCTION

Global warming is one of the most challenging issues of our time, and affects the natural environment, ecosystems, economies, and health. Human activities, mainly those involving the combustion of fossil fuels, have caused an increase in greenhouse gases (GHGs) that has resulted in a rise in global temperatures (WBCSD, 2004). CO_2 is the principal GHG emitted. In 2003, the transport sector was responsible for 24% of global CO_2 emissions (ECMT, 2007). Road surface transport accounts for more than three-quarters of transport-related CO_2 emissions (IEA, 2006), and this figure may be even higher in developed countries (ECMT, 2007). It is in the interests of all to reduce traffic-related emissions by increasing fuel efficiency through advances in vehicle design and transportation management policies that change travel behavior. This study focuses on the latter option.

Many studies have attempted to analyze the influences of travel patterns and transportation system design on transport emissions. They trace the cause and effect relationships of factors such as transport network topology, transport cost structure, congestion pricing regimes, traffic control methods, vehicular speed, road environment, the design and maintenance of road networks, travel demand structure, and traffic intensity on transport emissions levels (Nagurney *et al*., 2010; Nagurney, 2000a; Yin and Lawphongpanich, 2006; WBCSD, 2004).

For instance, an analytical framework has been established to decompose the transport emissions problem into the dimensions of population, transport intensity, energy intensity, and carbon intensity. This approach allows the aggregated effect of traveler activities, vehicle design, and fuel technologies on transport emissions to be estimated for different transport sub-sectors (Yang *et al*., 2009; Chiou and Chen, 2010).

Land-use patterns and transport planning policies affect transport demand and travel intensity. Earlier studies have identified the influence of land use and socioeconomic characteristics such as residential density, mixed land-use, car ownership levels, commuting distances, employment centre density, job-housing balance, and neighborhood design on the amount of travel activity (Cervero, 1996; Ewing, 1995; McNally and Kulkarni, 1997; Messenger and Ewing, 1996; Nowlan and Stewart, 1991; Cervero, 1989). Case studies have also been conducted to review the effects of transport policies such as alternative transport modes, transit systems, and vehicle emission permits on transport emissions in cities in Asia, Europe, and North America (Nagurney, 2000a; Nagurney, 2000b; Nagurney and Ramanujam, 1998; Poudenx, 2008).

However, these studies have all approached the transport emissions problem in a discrete manner. This means that weaknesses may have been introduced because of the data and methodology used. For instance, these studies are unable to account for the interactions among urban form, relevant factors, and transport intensity given the non-homogenous neighborhood, land-use, and socioeconomic characteristics of urban forms. An alternative for better understanding the relationships between land-use, transport planning, policy implementation, energy consumption, and transport emissions is an integrated transportation-land use approach (Boarnet and Crane, 2001; Badoe and Miller, 2000). For instance, a case study was carried out in Seattle to quantify the interactions among land use, travel choices, and vehicle emissions. The study offered an efficient and effective model of integrated land-use, transportation, and vehicle emissions patterns, and reduced the complexity of the problem through the use of indirect discrete models (Frank *et al*., 2000). Simulation models have also been established to examine the effect of land-use policies on transport activities and vehicle emissions. The factors investigated include rent control, land supply control, mixing residential and commercial use, carbon taxes, variable user charges, public transit system design, mixed motorized and non-motorized transport patterns, and route capacity (Hensher, 2008; Lam and Niemeier, 2005).

In this study, the integrated land-use, transport, and emissions problem is tackled by using a continuum model (Wong, 1998; Wong *et al*., 1998). In an earlier attempt, Ho and Wong (2005) formulated a continuum model to establish the relationship between transport demand and capacity and intensity in a transportation system. The finite element method (FEM) was applied to solve various transport-related optimization problems given a dense transportation network within a region of arbitrary shape. They then applied the continuum model to tackle a bi-level land-use and transportation optimization problem in which the negative utility of both housing rent and travel cost were minimized (Ho and Wong, 2007). In this study, the bi-level continuum transportation modeling approach is extended to solve the transport emissions problem given an optimized housing allocation pattern and minimum CO_2 emissions level. Some typical modeling approaches to transport emissions problems are first reviewed (Section 2). Then, the formulation of the proposed bi-level continuum model is described, with the user equilibrium achieved in the lower level and the housing allocation optimized in

the upper level (Section 3). Finally, a numerical example is given to demonstrate the applicability of the proposed model given a multi-class commuter scenario (Section 4). Finally, some concluding remarks are given (Section 5).

2. MODELING APPROACHES

In the literature, models of transport emissions problems can be classified into three categories. The first comprises the emission factor models, in which an emission factor is derived from the mean value of repeated measurements of total emissions per driving cycle. Two commonly used US transport emission models – MOBILE (EPA, 1994) and MOBILE (CARB, 2001) – fall into this category, in which the baseline emission rates are derived from a standard US laboratory test procedure, the Federal Test Procedure (FTP). Correction factors are established to incorporate the influence of factors such as vehicular speed, temperature, fuel type, and vehicle age on the baseline emission rates. Emission factor models provide a simple way to model area-wide vehicle emission levels, as less detailed information on traffic flow and operation pattern is required. However, the weakness of this modeling approach is its inability to account for the effects of vehicle operation states and driving environment on emission rates. The second category comprises the physical power-demand models, which can predict second-by-second tailpipe emissions for different driving conditions and vehicle types. A research team at the University of California, Riverside established the Comprehensive Modal Emission Model (CMEM) (An *et al*., 1997; Barth *et al*., 1996; Scora and Barth, 2006), which determines the vehicle emission rate as a function of vehicle operation characteristics, such as engine power, engine speed, air/fuel ratio, fuel use, engine-out emissions, and catalyst pass fraction, for each of the six vehicle operation modes. This modeling approach incorporates the effects of vehicle operation and driving environment into the emissions model, and thus provides a more accurate estimate of vehicle emission levels. However, detailed information on the operational characteristics at different vehicle speeds and acceleration rates and for different vehicle types is required. As these are usually difficult to obtain, this hinders the application of these models. The third category comprises the acceleration and speed-based models, in which emissions are defined as a function of vehicle type, instantaneous speed, and acceleration. Earlier versions of these models derived the average emission rate based on estimates of fourteen typical driving modes (Joumard *et al*., 1995). The emission rate is then denoted as a function of a combination of linear, quadratic, and cubic transforms of the instantaneous speed and acceleration, which can readily be derived from data on the average speed and number of stops of the specified driving mode (Ahn *et al*., 1999; Ahn *et al*., 2002; Rakha *et al*., 2004). This modeling approach is promising, as less detailed engine operation and driving environment information are required (compared with the physical power-demand models) and the influence of vehicle movement is controlled (which is not the case in the emission factor models) (Dion *et al*., 2000).

The acceleration and speed-based modeling approach is applied to estimate the transport emissions rate with a bi-level continuum transportation model given optimized housing allocation, user equilibrium, and minimized CO_2 emissions. The use of this emissions modeling approach in a continuum transportation system is appealing, as the difference in link characteristics between adjacent areas is small compared with the entire territory in a hypothetical transport system. Although the acceleration and speed-based models are efficient, the continuum transportation model for integrated land-use and transportation problems offers

the additional strengths of suitability for the initial phase of planning and broad-scale regional studies, and better modeling of the general trends and distribution patterns at the macroscopic level. The proposed model should also significantly reduce the model and problem size and the data required through the use of abstract mathematical functions.

3. METHODOLOGY

3.1 Lower-level Subprogram

3.1.1 Model formulation

In this section, a city of arbitrary shape with one central business district (CBD), as shown in Figure 1, is studied. The road network outside the CBD is assumed to be relatively dense and can be considered as a continuum. Transport demand and housing are continuously distributed over the region outside the CBD, and all of the employment is concentrated in the CBD, and road users should arrive at the CBD at a uniform rate. Commuters travel between their homes and the CBD along the least costly route during the morning peak hour every day. Several classes of commuters with different types of behavior and perceptions are considered in the housing allocation model. We denote the region of the city as Ω, the outer boundary of the city as Γ, the location of the CBD as O, and the boundary of the CBD as Γ_c. It is assumed that no commuters will travel across the outer boundary (Γ) of the city, and that all of the activity is concentrated within the CBD.

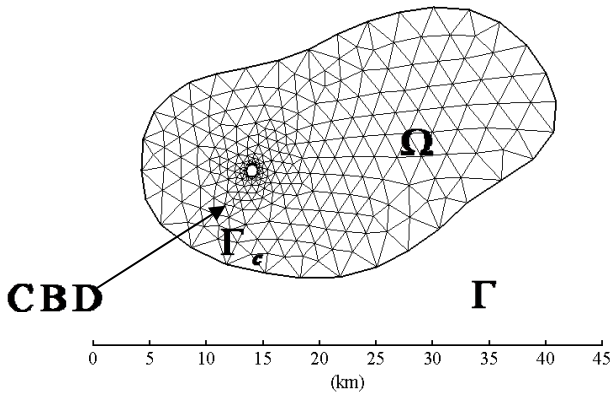

Figure 1. Modeled city with an arbitrary shape and the finite element mesh generated

At location (x, y), $\mathbf{f}_m(x, y) = (f_{mx}(x, y), f_{my}(x, y))$ is defined as the flow vector of class m commuters (expressed as the number of commuters that cross a unit width), where $f_{mx}(x, y)$ and $f_{my}(x, y)$ are the flow flux in the x-direction and y-direction. $|\mathbf{f}_m(x, y)| = \sqrt{f_{mx}(x, y)^2 + f_{my}(x, y)^2}$ is then the flow intensity of class m commuters. At a particular location (x, y) and for a given flow pattern $\mathbf{f}_m(x, y)$, the speed is defined as a monotonic decreasing function of the total flow intensity $v(x, y) = g\left(\sum_{m=1}^{N_m} |\mathbf{f}_m(x, y)|\right)$. To take into consideration the relationship between acceleration and speed, which is easy to find, the following equations must be satisfied.

$$a_{mx}(x, y) - v_{mx}(x, y)\frac{\partial v_{mx}(x, y)}{\partial x} = 0, \forall (x, y) \in \Omega, m \in N_m, \quad (1)$$

$$a_{my}(x,y) - v_{my}(x,y)\frac{\partial v_{my}(x,y)}{\partial y} = 0, \forall (x,y) \in \Omega, m \in N_m, \quad (2)$$

where $\mathbf{a}_m(x,y) = (a_{mx}(x,y), a_{my}(x,y))$ is the acceleration vector of class m commuters, a_{mx} and a_{my} are the accelerations in the x-direction and y-direction, respectively, for class m commuters, $v_{mx}(x,y) = v(x,y) f_{mx}(x,y) / |\mathbf{f}_m(x,y)|$ and $v_{my}(x,y) = v(x,y) f_{my}(x,y) / |\mathbf{f}_m(x,y)|$ are the speeds in the x-direction and y-direction, respectively, for class m commuters, and N_m is the total number of classes. The travel cost potential is defined next. Let $c(x,y)$ be the local travel cost, which is related to the travel speed as

$$c(x,y) = 1/v(x,y), \quad (3)$$

where the travel cost is expressed in hours per unit length of travel at location (x,y). As travel speed is a monotonic decreasing function of the total flow intensity, a BPR-type relationship is defined between local travel cost and traffic intensity, as follows.

$$c(x,y) = c_0(x,y) + \eta(x,y)\left(\sum_{m=1}^{N_m} |\mathbf{f}_m(x,y)|\right)^{\gamma}, \forall (x,y) \in \Omega, \quad (4)$$

where $c_0(x,y)$ is the free-flow travel time and $\eta(x,y)$ is the congestion sensitivity parameter at location (x,y). Let p_m be the value of time for class m commuters. The travel cost of class m commuters can be expressed in dollars per unit length of travel at (x,y) as

$$c_m(x,y) = p_m c(x,y), \forall (x,y) \in \Omega, m \in N_m. \quad (5)$$

For a given flow pattern $\mathbf{f}_m(x,y)$ and the unit travel cost $c_m(x,y)$, the function $u_m(x,y)$ is considered, which is the total travel cost of class m commuters at location (x,y) to travel to the CBD.

$$c_m(x,y)\frac{f_{mx}(x,y)}{|\mathbf{f}_m(x,y)|} + \frac{\partial u_m(x,y)}{\partial x} = 0, \forall (x,y) \in \Omega, m \in N_m, \quad (6)$$

$$c_m(x,y)\frac{f_{my}(x,y)}{|\mathbf{f}_m(x,y)|} + \frac{\partial u_m(x,y)}{\partial y} = 0, \forall (x,y) \in \Omega, m \in N_m. \quad (7)$$

These equations have been proven to guarantee that commuters will choose the least costly route over the city region in a user-optimal manner (Ho and Wong, 2005; Ho and Wong, 2007). For each class of commuter, the flow vector and trip demand must satisfy the flow conservation conditions in the region of the city.

$$\nabla \mathbf{f}_m(x,y) - q_m(x,y) = 0, \forall (x,y) \in \Omega, m \in N_m, \quad (8)$$

where $\nabla \mathbf{f}_m(x,y) = \frac{\partial f_{mx}}{\partial x} + \frac{\partial f_{my}}{\partial y}$ is the gradient of the flow vector $\mathbf{f}_m(x,y)$ and $q_m(x,y)$ is the density of the demand of class m commuters at location (x,y) (expressed as the number of commuters per unit area).

The interaction between housing allocation and traffic equilibrium is governed by the demand distribution function, which is used to describe the way in which commuters choose the location of their home in the city. Ho and Wong (Ho and Wong, 2005; Ho and Wong, 2007) identified housing rent and travel cost to be the basic variables that affect commuters' choice of where to live. The following equation is used to incorporate the housing allocation problem into the transportation equilibrium problem.

$$q_m(x,y) - Q_m \frac{\exp(\gamma_m U_m(q(x,y),u_m(x,y)))}{\iint_\Omega \exp(\gamma_m U_m(q(x,y),u_m(x,y)))d\Omega} = 0, \forall (x,y) \in \Omega, m \in N_m, \quad (9)$$

where Q_m is the total demand of class m commuters, $U_m(q(x,y),u_m(x,y))$ is the utility function perceived by class m commuters at location (x,y), and γ_m is a positive scalar parameter that measures the sensitivity of class m commuters to the utility level associated with location (x,y).

$$U_m(q(x,y),u_m(x,y)) = -u_m(x,y) - \bar{r}_m(x,y).$$

The utility function consists of two components. The second term is the housing rent, which depends on the total demand density $q(x,y) = \sum_{m=1}^{N_m} q_m(x,y)$ and the total housing supply density $H(x,y)$,

$$\bar{r}_m(x,y) = \alpha_m(x,y)(1+\beta_m(x,y)q(x,y)/(H(x,y)-q(x,y))), \quad (10)$$

where $\alpha_m(x,y)$ and $\beta_m(x,y)$ are scalar parameters that represent the fixed and demand-dependent components of the rent function at location (x,y).

The boundary conditions that must be satisfied are also considered.

$$u_m = 0, \forall (x,y) \in \Gamma_c, \forall m \in N_m, \quad (11)$$

$$\mathbf{f}_m = 0, \forall (x,y) \in \Gamma, \forall m \in N_m, \quad (12)$$

In equation (11), as users at Γ_c are already at the boundary of the CBD, they will incur no transportation cost in traveling to the CBD. In equation (12), it is assumed that no commuters travel across the outer boundary of the city Γ. Thus, the flow should be zero and the total demand across the city should be fixed.

3.1.2 Solution algorithm

The finite element method (FEM) is used to solve the problem. This involves five steps: 1) discretization of the modeled city into finite elements; 2) description of the equations that the variables must satisfy at each node; 3) assembly of the equations; 4) introduction of the boundary conditions that must be satisfied; and, 5) solution of the system of equations.

The Galerkin formulation of the weighted residual technique is adopted to transform the differential equations (1), (2), (6), (7), (8), and (9) into the following expressions, where $\Psi(x,y)$ is the weight function in the weighted residual technique and can take any value.

$$\iint_\Omega (a_{mx}(x,y) - v_{mx}(x,y)\frac{\partial v_{mx}(x,y)}{\partial x})\Psi(x,y)d\Omega = 0, \forall m \in N_m, \Psi(x,y), \quad (13)$$

$$\iint_\Omega (a_{my}(x,y) - v_{my}(x,y)\frac{\partial v_{my}(x,y)}{\partial y})\Psi(x,y)d\Omega = 0, \forall m \in N_m, \Psi(x,y), \quad (14)$$

$$\iint_\Omega (c_m(x,y)\frac{f_{mx}(x,y)}{|\mathbf{f}_m(x,y)|} + \frac{\partial u_m(x,y)}{\partial x})\Psi(x,y)d\Omega = 0, \forall m \in N_m, \Psi(x,y), \quad (15)$$

$$\iint_\Omega (c_m(x,y)\frac{f_{my}(x,y)}{|\mathbf{f}_m(x,y)|} + \frac{\partial u_m(x,y)}{\partial y})\Psi(x,y)d\Omega = 0, \forall m \in N_m, \Psi(x,y), \quad (16)$$

$$\iint_\Omega (\nabla \mathbf{f}_m(x,y) - q_m(x,y))\Psi(x,y)d\Omega = 0, \forall m \in N_m, \Psi(x,y), \quad (17)$$

$$\iint_{\Omega}(q_m(x,y)-\frac{Q_m\times\exp(\gamma_m U_m(q(x,y),u_m(x,y)))}{\iint_{\Omega}\exp(\gamma_m U_m(q(x,y),u_m(x,y)))d\Omega})\Psi(x,y)d\Omega=0,\forall m\in N_m,\Psi(x,y),(18)$$

After the region is discretized, the local interpolation function $N(x,y)$ can be forced to $\Psi(x,y)$, because $\Psi(x,y)$ can be any value. For a specific node s, the governing equations for all classes of commuters are given as follows.

$$\mathbf{r}_{sm}(\mathbf{\Psi})=\left\{\begin{array}{c}\sum_{e\in T_s}\iint_{\Omega_e}(a_{mx}(x,y)-v_{mx}(x,y)\frac{\partial v_{mx}(x,y)}{\partial x})N_s(x,y)d\Omega\\ \sum_{e\in T_s}\iint_{\Omega_e}(a_{my}(x,y)-v_{my}(x,y)\frac{\partial v_{my}(x,y)}{\partial y})N_s(x,y)d\Omega\\ \sum_{e\in T_s}\iint_{\Omega_e}(c_m(x,y)\frac{f_{mx}(x,y)}{|\mathbf{f}_m(x,y)|}+\frac{\partial u_m(x,y)}{\partial x})N_s(x,y)d\Omega\\ \sum_{e\in T_s}\iint_{\Omega_e}(c_m(x,y)\frac{f_{my}(x,y)}{|\mathbf{f}_m(x,y)|}+\frac{\partial u_m(x,y)}{\partial y})N_s(x,y)d\Omega\\ \sum_{e\in T_s}\iint_{\Omega_e}(\nabla\mathbf{f}_m(x,y)-q_m(x,y))N_s(x,y)d\Omega\\ \sum_{e\in T_s}\iint_{\Omega_e}(q_m(x,y)-\frac{Q_m\times\exp(\gamma_m U_m(q(x,y),u_m(x,y)))}{\iint_{\Omega}\exp(\gamma_m U_m(q(x,y),u_m(x,y)))d\Omega})N_s(x,y)d\Omega\end{array}\right\},(19)$$

where Ω_e denotes the region of the elements e, T_s is the set of elements that connects with node s, $N_s(x,y)$ is the local interpolation function of the element that connects with node s. $\mathbf{r}_{sm}$ is the nodal residual vector for class m commuters at node s. $\mathbf{r}_{sm}=0$ means that the governing equations (1), (2), (6), (7), (8), and (9) can be locally satisfied. For the global satisfaction of the governing equations, it is required that

$$\mathbf{R(\Psi)}=\mathrm{Col}(\mathbf{r_{sm}(\Psi)})=0. \quad (20)$$

Boundary conditions (11) and (12) can be satisfied by forcing the specific variables to take a known value, which is very common in FEM. For this system of non-linear equations, the Newton-Raphson algorithm can be applied with a line search to find a solution, for which the iterative equation is derived

$$\mathbf{\Psi}_{k+1}=\mathbf{\Psi}_k-\lambda\mathbf{J}_k^{-1}\mathbf{R}_k, \quad (21)$$

where $\mathbf{J}_k$ is the Jacobian matrix of vector $\mathbf{R}_k$ at iteration k and λ is the step size, which is obtained by a line search to achieve the minimum $|\mathbf{R(\Psi)}|$. The relative error $|\mathbf{R(\Psi)}|/|\mathbf{\Psi}|$ is compared with the acceptable threshold ε. If $|\mathbf{R(\Psi)}|/|\mathbf{\Psi}|<\varepsilon$, then it is assumed that the solution to the system of equations (equation 20) is found. The solution procedure is summarized as follows.

Solution Procedure A

Step A1: Find an initial solution $\mathbf{\psi}_0$. Set $k=0$.

Step A2: Evaluate $\mathbf{R(\psi}_k\mathbf{)}$ and $\mathbf{J(\psi}_k\mathbf{)}$.

Step A3: If the relative error $|\mathbf{R(\Psi}_k\mathbf{)}|/|\mathbf{\Psi}_k|$ is less than the accepted error ε, then stop, and take $\mathbf{\Psi}_k$ as the solution.

Step A4: Otherwise, apply the golden section method (with the smallest search interval of δ) to determine the step size λ^* that minimizes the norm of the residual vector $|\mathbf{R}(\mathbf{\Psi}_{k+1} - \lambda \mathbf{J}_k^{-1}\mathbf{R}_k)|$. Then, set $\mathbf{\Psi}_{k+1} = \mathbf{\Psi}_k - \lambda^* \mathbf{J}_k^{-1}\mathbf{R}_k$.
Step A5: Replace $\mathbf{\Psi}_k$ with $\mathbf{\Psi}_{k+1}$. Set $k = k+1$, and go to *Step A2*.

3.2 Upper-level Subprogram

3.2.1 Model formulation

This section introduces the upper-level subprogram of the land-use and transportation problem, which aims to find the optimal housing provision pattern that will result in the largest reduction in total CO_2 emissions during peak hours for a given total travel demand and budgetary constraint. The minimization problem of the upper level is modeled as follows.

$$\underset{\mathbf{h}}{Minimize}\ \ z(\mathbf{h}) = \sum_{m=1}^{N_m} \iint_{\Omega} \left|\mathbf{f}_{\mathbf{m}}^*(x,y)\right| E_{\mathrm{CO2}}^m \left(\mathbf{f}_1^*(x,y), \cdots, \mathbf{f}_{N_m}^*(x,y), \mathbf{a}_m^*(x,y)\right) / v^*(x,y)\, \mathrm{d}\Omega \quad (22)$$

subject to

$$H_{\max}(x,y) - (h_0(x,y) + h(x,y)) \geq 0, \forall (x,y) \in \Omega, \quad (23)$$

$$h(x,y) \geq 0, \forall (x,y) \in \Omega, \quad (24)$$

$$B - \iint_{\Omega} P(x,y) h(x,y) d\Omega \geq 0, \forall (x,y) \in \Omega, \quad (25)$$

$$\iint_{\Omega} h(x,y) + h_0(x,y) - q^*(x,y)\, \mathrm{d}\Omega \geq 0, \forall (x,y) \in \Omega, \quad (26)$$

where $h_0(x,y)$ is the existing housing provision and $h(x,y)$ is the additional housing provision at a particular location (x,y). $H_{\max}(x,y)$ is the maximum possible housing density at location (x,y), which is constrained by topography, the existing transportation infrastructure, and the planned land-use pattern. B is the budget that is available for additional housing provision, and $P(x,y)$ is the cost of building a housing unit at location (x,y). The superscript (*) denotes variables that are the optimal solution from the lower-level subprogram. In terms of the constraints, equation (23) ensures that the total housing development should not exceed the maximum possible housing density. Constraint (24) means that there will not be any demolition of the existing housing supply. Constraint (25) states that the total investment in housing provision cannot exceed budget B. Constraint (26) guarantees that there is sufficient housing provision for commuters.

E_{CO2}^m is the CO_2 emission rate function for class m users, which is derived using an acceleration and speed based model. The emission mode proposed by Ahn *et al*. (2002) is adopted to estimate the emission rate of each class of users, as follows.

$$E_e = \exp\left(\sum_{i=0}^{3}\sum_{j=0}^{3} k_{i,j}^e v^i a^j\right), \quad (27)$$

where a is the instantaneous acceleration (m/s^2), v is the instantaneous speed (km/h), $k_{i,j}^e$ is the model regression coefficient for speed power i and acceleration power j, and E_e is the instantaneous fuel consumption and emission rate, with the subscript (e) denoting different kinds of emissions, including CO, NO, CO_2 (mg/s), and fuel consumption (l/s).

Under the route choice governed by the user-optimal conditions, commuters may accelerate or decelerate along their trajectory according to the spatial variation in traffic conditions in the

neighboring area. To identify whether acceleration or deceleration occurs, the following expression is used to determine the acceleration in the movement direction of commuters,

$$a = (a_x f_x + a_y f_y) / \sqrt{f_x^{\,2} + f_y^{\,2}} \ . \tag{28}$$

Based on the limited parameters (can be found in (Ahn *et al*., 1999)), this model cannot be used directly, as only existing parameters are for HC, NO, and estimated fuel consumption. However, the CO_2 emissions function, which is shown in equation (29) can be derived based on the carbon balance between the fuel consumption and emissions.

$$E^{\mathrm{CO2}} = 2458.29F - 3.17E^{\mathrm{HC}} - 1.57E^{\mathrm{CO}}, \tag{29}$$

$$F = \exp\left(\sum_{i=0}^{3}\sum_{j=0}^{3} k_{i,j}^{1} v^i a^j\right), E^{\mathrm{CO}} = \exp\left(\sum_{i=0}^{3}\sum_{j=0}^{3} k_{i,j}^{2} v^i a^j\right), E^{\mathrm{HC}} = \exp\left(\sum_{i=0}^{3}\sum_{j=0}^{3} k_{i,j}^{3} v^i a^j\right) \tag{30}$$

F is fuel consumption (*gal/h*), and E^{HC}, E^{CO}, E^{CO2} are the relative gas emission rates (*mg/s*).

3.2.2 Solution algorithm

The minimization problem is non-linear, and thus to reduce the difficulty of solving it we first use the FEM to transform constraints (25) and (26) into linear ones.

$$B - \sum_{n=1}^{N_{FN}} (h_n \sum_{e \in \Omega_{en}} \iint_{\Omega_e} (P_{ei} N_i N_n + P_{ej} N_j N_n + P_{ek} N_k N_n) d\Omega) \geq 0, \tag{31}$$

$$\frac{1}{3}\sum_{n=1}^{N_{FN}} \Delta_n h_n + \frac{1}{3}\sum_{n=1}^{N_{FN}} \Delta_n (h_n^0 - q_n^*) \geq 0, \tag{32}$$

where N_{FN} is the total number of finite elements nodes within the generated mesh, N_j is the interpolation function of the FEM for node i, P_{ei} is the cost of building a housing unit at node i within element e, Δ_n is the area of the finite elements that connect with node n, Ω_e is the region of element e, Ω_{en} is the region that connects with node n, h_n^0 and h_n are the existing and additional housing provision at node n, and q_n^* is the total demand at node n obtained from the lower-level subprogram.

Based on the convex combination method and constraints (23), (24), (31), and (32), a linear optimization problem can be set up as follows.

$$\underset{\mathbf{w}}{Minimize} \nabla z(\mathbf{h}) \cdot \mathbf{w} \tag{33}$$

subject to

$$H_{\max} - (h_n^0 + w_n) \geq 0, \forall n \in N_{FN}, \tag{34}$$

$$w_n \geq 0, \forall n \in N_{FN}, \tag{35}$$

$$B - \sum_{n=1}^{N_{FN}} (w_n \sum_{e \in \Omega_{en}} \iint_{\Omega_e} (P_{ei} N_i N_n + P_{ej} N_j N_n + P_{ek} N_k N_n) \mathrm{d}\Omega) \geq 0, \tag{36}$$

$$\frac{1}{3}\sum_{n=1}^{N_{FN}} \Delta_n w_n + \frac{1}{3}\sum_{n=1}^{N_{FN}} \Delta_n (h_n^0 - q_n^*) \geq 0, \tag{37}$$

where $\mathbf{h} = (h_1, \cdots, h_{N_{FN}})$ is the current housing allocation vector and $\mathbf{w} = (w_1, \cdots, w_{N_{FN}})$ is a feasible solution that falls into the region governed by constraints (34), (35), (36) and (37). $\mathbf{w} - \mathbf{h}$ is the descent direction for the minimization problem (22). A line search is used to find a step that will guarantee the largest descent.

However, to solve this problem, the gradient of the object function $z(\mathbf{h})$ and the sensitivity of the lower-level variables ($f_{mx}^*, f_{my}^*, u_m^*, q_m^*, a_{mx}^*, a_{my}^*$) to the upper-level variables ($\mathbf{h}$) must be found. By denoting the lower-level and upper-level variables as $\mathbf{\Psi}_l^*$ and $\mathbf{\Psi}_u^*$ respectively, equation (20) can be modified to

$$\mathbf{R}(\mathbf{\Psi}_l^*, \mathbf{\Psi}_u) = 0 . \tag{38}$$

Taking a partial derivative of $\mathbf{\Psi}_u$ of the left-hand side of equation (38) will result in

$$\nabla_{\mathbf{\Psi}_u} \mathbf{\Psi}_l^* = -J(\mathbf{\Psi}_l^*, \mathbf{\Psi}_u)^{-1} \nabla_{\mathbf{\Psi}_u} R(\mathbf{\Psi}_l^*, \mathbf{\Psi}_u) . \tag{39}$$

Equation (39) is the matrix of the sensitivity of the optimized lower-level variables ($\mathbf{\Psi}_l^*$) to the upper-level variables ($\mathbf{\Psi}_u$), and can be found for each solution of the lower-level subprogram. Using the sensitivity matrix in equation (39), the direction of descent of the minimization problem (22) can be found by solving linear program (33). The following solution procedure is adopted to solve the problem.

Solution Procedure B

Step B1: Set $k = 1$. Take the initial solution for the upper level to be $\mathbf{\Psi}_{u1} = \mathbf{h}_1 = 0$.

Step B2: With $\mathbf{\Psi}_{uk}$, solve the lower-level subprogram, which is based on solution procedure A, to find the solution for the lower-level $\mathbf{\Psi}_{lk}$.

Step B3: Using $\mathbf{\Psi}_{lk}$, evaluate the sensitivity matrix according to equation (39).

Step B4: Use the sensitivity matrix from the lower level to find auxiliary vector $\mathbf{w}_k$.

Step B5: Apply the golden section method (with the smallest search interval of δ) to find the step size $\lambda_k^* \in [0,1]$ that maximizes the objective function $z(\mathbf{h}_k + \lambda_k^*(\mathbf{w}_k - \mathbf{h}_k))$ from equation (22). Then, set $\mathbf{d}_k = \mathbf{h}_k + \lambda^*_k(\mathbf{w}_k - \mathbf{h}_k)$.

Step B6: If $z(\mathbf{d}_k) > z(\mathbf{h}_k)$, then set $\mathbf{h}_{k+1} = \mathbf{d}_k$, $k = k+1$ and go to *Step B2*; otherwise stop and take $\mathbf{h}_k$ as the solution to the upper-level subprogram and $\mathbf{\Psi}_{lk}$ as the corresponding solution to the lower-level subprogram.

4. NUMERICAL EXAMPLE

A numerical example is given to demonstrate how the bi-level model works for the optimization of the housing allocation problem. The example considers a city of arbitrary shape, as shown in Figure 1. The city spans about 35 km. from east to west and 25 km. from north to south. Its CBD is located at the southwestern area of the city. The finite element mesh generated for solving the problem is also shown in Figure 1.

In this example, two classes of commuters are considered. The population of class 1 commuters is 60,000 units and that of class 2 commuters is 80,000 units. It is assumed that all commuters will travel to the CBD during the morning peak hour and return home along the reverse route during the evening peak hour. The travel cost represents the sum of the travel cost in each period, and can be interpreted as the cost of travel at that specific location. The

sensitivity parameters for the housing choice functions in equation (9) are 0.0015 and 0.0020 for the class 1 and class 2 commuters, respectively. The unit travel time function is

$$c(x,y) = 0.0125 + 2.0\times10^{-6}\left(\left|\mathbf{f}_1(x,y)\right| + \left|\mathbf{f}_2(x,y)\right|\right)^{1.2}, \forall (x,y) \in \Omega .$$

The instantaneous speed function is then:

$$\left|v(x,y)\right| = 1/c(x,y) = 1/\left(0.0125 + 2.0\times10^{-6}\left(\left|\mathbf{f}_1(x,y)\right| + \left|\mathbf{f}_2(x,y)\right|\right)^{1.2}\right),$$

where $c(x,y)$ is measured in hours per kilometer and $\mathbf{f}_1 = (f_{x1}, f_{y1})$ and $\mathbf{f}_2 = (f_{x2}, f_{y2})$ are the flow vectors of class 1 and class 2 commuters at location (x,y). The value of time p_m for class 1 and class 2 commuters is 50 HKD/h and 75 HKD/h, respectively. The housing rent functions are

$$\text{Class 1 commuter: } \overline{r_1} = 40(1 + 20\,p/(H-p)),$$

$$\text{Class 2 commuter: } \overline{r_2} = 40(1 + p/(H-p)),$$

where $\overline{r_1}$ and $\overline{r_2}$ are measured in HKD. Class 1 commuters are more sensitive to housing rent then class 2 commuters, which means that they place a greater value on housing rent when making a decision about where to live. In contrast, class 2 commuters value the time cost of transportation more, and are thus more sensitive to time.

The existing housing unit h_{0n} is assumed to be taken as a constant of 350 units per km^2 over the whole city. The maximum possible housing development is assumed to be 600 units per km^2, respectively, for all locations (x,y). The budget that is available for additional housing units is assumed to be 1 billon HKD, and the unit provision cost function is

$$P(x,y) = 10000(1.50 - 0.005\sqrt{(x-14)^2 + (y-20)^2}),$$

where $P(x,y)$ is measured in HKD and (14, 20) is the location of the center of the CBD. This function increases as the distance from the CBD decreases, as it is assumed that the cost of land acquisition is higher near the CBD.

By taking the acceptable error $\varepsilon = 10^{-7}$ for the lower-level model and the smallest search interval $\delta = 0.02$ for the golden section method in both the lower-level and upper-level model, this numerical example can be solved in four iterations, which takes approximately four hours using a personal computer with an E8400 3.00GHz CPU and 3.12GB of RAM. The convergence curve for the housing provision model is shown in Figure 2.

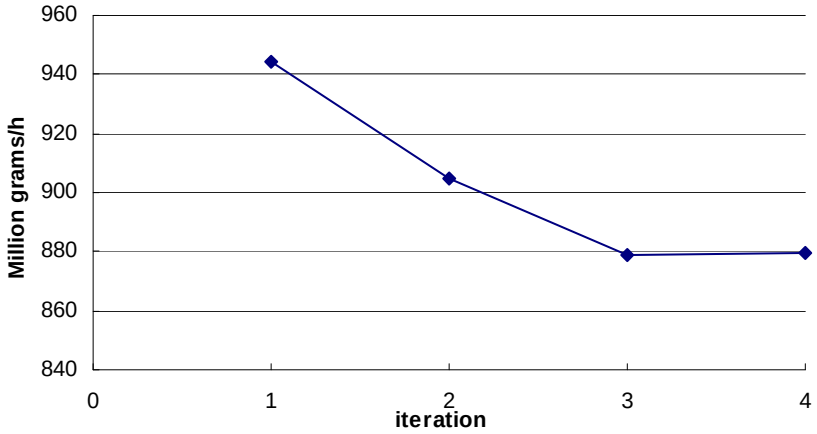

Figure 2. Typical convergence plot for the solution

Figure 3a shows the flow trajectories of Class 2 commuters traveling from their housing location to the CBD. The trajectory curve guarantees the user equilibrium conditions. The flow intensity and the travel cost for Class 2 commuters after the upper-level optimization are shown in Figures 3b and 3c. The total flow intensity decreases and travel cost increases as the distance from the CBD increases. The flow trajectories, flow intensity, and total travel cost for Class 1 commuters are not shown, as they are quite similar to those of Class 2 commuters. The total flow intensity pattern is similar to that in Figure 3b, and based on equation (1), it can be determined that the speed decreases as the distance from the CBD decreases.

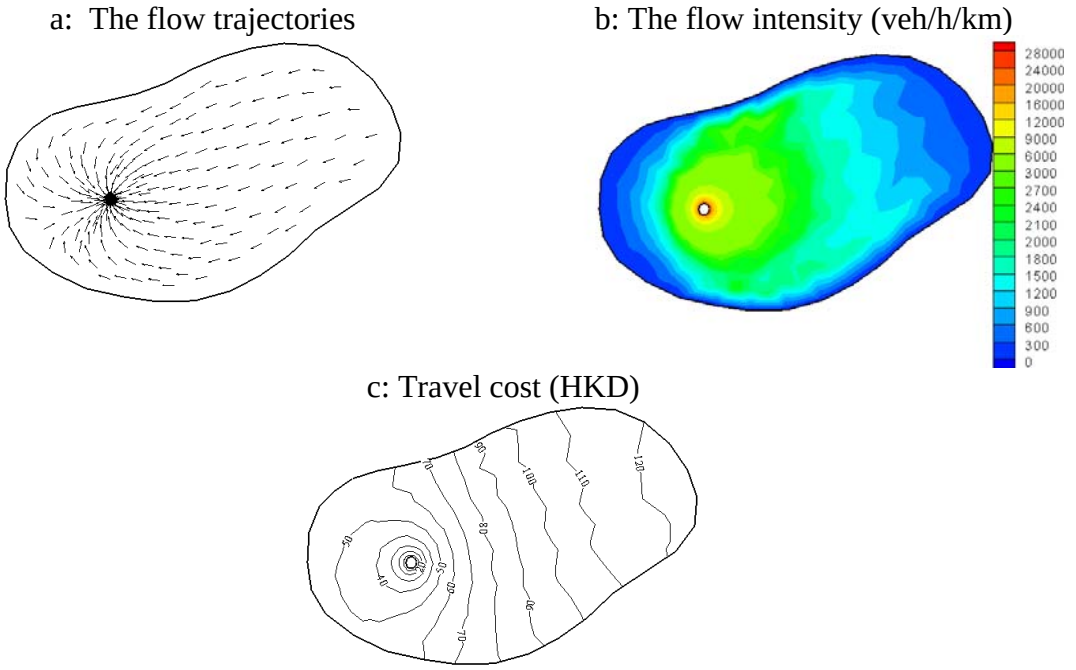

Figure 3. Flow pattern of class 2 commuters and the travel cost after the optimization

Figure 4 shows the changes in demand distribution for both classes of commuters arising from additional housing provision, which indicates that class 2 commuters are less sensitive to housing rent and value travel cost more, and thus tend to live closer to the CBD than class 1 commuters. Moreover, the added housing units are mostly occupied by the class 1 commuters, which is consistent with the conclusion that class 1 commuters are more sensitive to housing rent.

Figure 5a shows the additional housing units when the total CO_2 emissions from the transportation sector are minimized. Figure 5a clearly shows that the additional housing units are mostly concentrated around the CBD, which is easy to understand. The factors that most influence transportation emissions are speed and acceleration. The CO_2 emissions produced increases as the acceleration changes from negative to positive, and both a high and a low speed result in more emissions than a moderate speed. However, as shown in the model, all of the commuters travel to the CBD during the morning peak, the total flow intensity in the areas adjacent to the CBD will not change much, regardless of how the additional housing units are distributed. If most of the housing units are concentrated around the CBD, then the speed around the CBD does not change much but commuters generally travel shorter distances, thus producing less emissions. It is widely believed that in the process of urbanization, developing

suburbs around a central CBD is better, especially for big cities with large populations. However, this result indicates that such urban sprawls introduce more long-distance travel to the central CBD every day. Both CO_2 emissions and congestion are greater.

a: Class 1 commuters before optimization

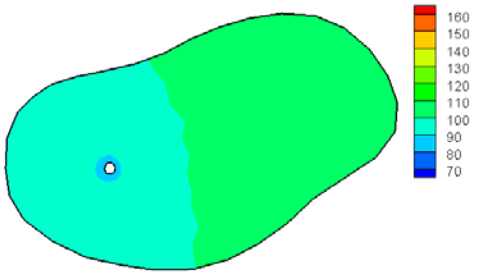

c: Class 1 commuters after optimization

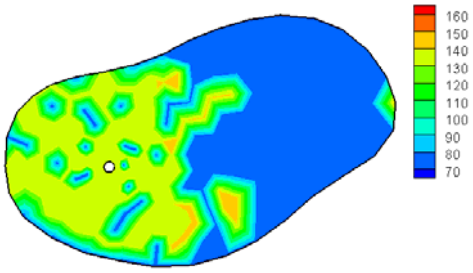

b: Class 2 commuters before optimization

d: Class 2 commuters after optimization

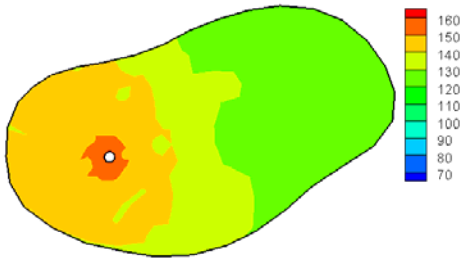

Figure 4. Demand contours (veh/h/km^2)

For traffic-related emissions, Figures 5c and 5d show that the emission rates increase sharply near the CBD for both classes of users, because of the significant reduction in speed due to severe traffic congestion. The emission rates in Figures 5c and 5d are not identical because, although the speed is the same for both classes, their flow trajectories are different, which affects the tangential acceleration in the emission rate estimation. Figure 5b shows the distribution of total emissions in the city by multiplying the flow intensities with the respective emission rates for both classes. Higher emission concentration occurs around the CBD due to more severe congestion there.

5. CONCLUSIONS

In this study, the continuum modeling approach is extended to solve a bi-level problem to optimize housing allocation to achieve minimum transport emissions in an integrated land-use and transportation modeling framework. At the lower-level, the transport equilibrium problem given the optimum utility of housing rent and travel cost is solved, and gives two commuter classes with different sensitivities. At the upper level, the optimal housing allocation pattern that minimizes total CO_2 emissions from the transportation sector during peak hours is determined, in which the objective function is derived by the instantaneous speed and acceleration of a given driving mode. By discretizing the constraints with FEM, the convex combination method is adopted as the solution algorithm for the problem. A numerical example is given to demonstrate the effectiveness of the solution algorithms for both the lower-level and upper-level subprograms. At the same time, there are several possible extensions to the proposed modeling approach that could be undertaken in future research on

the transport emissions problem. For instance, the model could be extended to a multiple CBD problem, in which commuters can choose their housing location in response to the employment opportunities offered in different CBDs. So far, the emissions problem using a static continuum model is studied, in which the CO_2 emission rate at peak hours can only be modeled. A dynamic continuum model could be established to incorporate the effects of multiple vehicle classes and time-varying transport demand on emission levels into the land-use transportation modeling framework. This modeling approach is particularly useful for highly populated cities in Asia, in which both population and road densities are high, and many of these cites are facing the challenging global issues of the ever increasing population, urbanization, climate change, resources depletion and environmental pollution. This methodology offers a qualitative diagnosis of the city development to reduce greenhouse emissions in this rapidly growing region.

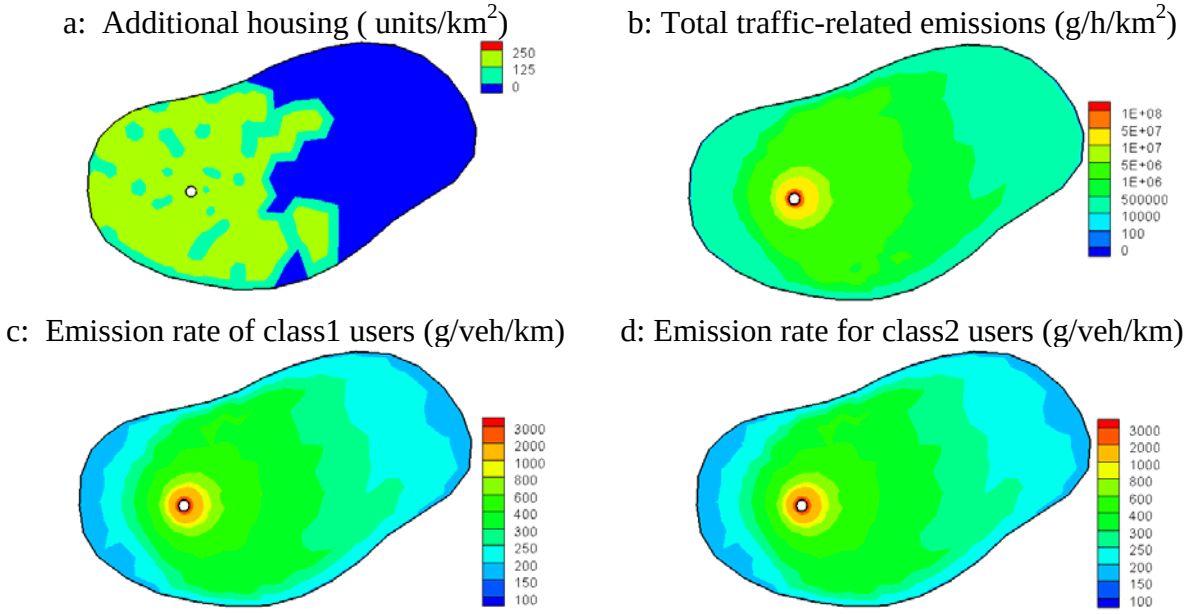

Figure 5. Emissions and additional housing distribution in the city

ACKNOWLEDGEMENTS

The work that is described in this paper was jointly supported by a Research Postgraduate Studentship, an Outstanding Researcher Award, and the Engineering Postdoctoral Fellowship Programme from the University of Hong Kong, and a grant from the Research Grants Council of the Hong Kong Special Administrative Region of China (Project No. HKU7183/08E).

REFERENCES

Ahn, K., Rakha, H., Trani, A., Van Aerde, M. (2002) Estimating vehicle fuel consumption and emissions based on instantaneous speed and acceleration levels. *ASCE Journal of Transportation Engineering*, 128 (2), 182-190.

Ahn, K., Trani, A., Rakha, H., Van Aerde, M. (1999) Microscopic fuel consumption and emission models. *Compendium of Papers CD-ROM, the 78th Annual Meeting of the Transportation Research Board*, Washington, D.C., January 10-14.

An, F., Barth, M., Norbeck, J., Ross, M. (1997) Development of comprehensive modal emissions model operating under hot-stabilized conditions. *Transportation Research Record*, 1587, 52-62.

Badoe, D.A., Miller, E.J. (2000) Transportation-land-use interaction: Empirical findings in North America, and their implications for modeling. *Transportation Research Part D*, 5 (4), 235-263.

Barth, M., An, F., Norbeck, J., Ross, M. (1996) Modal emissions modeling: A physical approach. *Transportation Resarch Record*, 1520, 81-88.

Boarnet, M., Crane, R. (2001) The influence of land use on travel behavior: Specification and estimation strategies. *Transportation Research Part A*, 35 (9), 823-845.

CARB (2001) *EMFAC2007 v2.3 User's Guide*, California Air Resources Board.

Cervero, R. (1989) *America's Suburban Centers: The Land-use-Transportation Link*, Unwin Hyman Inc.

Cervero, R. (1996) Mixed land-uses and commuting: Evidence from the American Housing Survey. *Transportation Research Part A*, 30 (15), 361-377.

Chiou, Y.-C., Chen, T.-C. (2010) Direct and indirect factors affecting emissions of cars and motorcycles in Taiwan. *Transportmetrica*, 6 (3), 215-233.

Dion, F., Van Aerde, M., Rakha, H. (2000) Mesoscopic fuel consumption and vehicle emission rate estimation as a function of average speed and number of stops. *Compendium of Papers CD-ROM, the 79th Annual Meeting of the Transportation Research Board*, Washington, D.C., January 9-13.

ECMT (2007) *Cutting Transport CO2 Emission: What Progress?*. European Conference of Ministers of Transport, Paris.

EPA (1994) *User's Guide to MOBILE5*. U.S. Environmental Protection Agency.

Ewing, R. (1995) Beyond density, mode-choice, and single-purpose trips. *Compendium of Papers CD-ROM, the 74th Annual Meeting of the Transportation Research Board*, Washington, D.C., January 22-28.

Frank, L. D., Stone, B., Bachman, W. (2000) Linking land use with household vehicle emissions in the central Puget Sound: Methodological framework and findings. *Transportation Research Part D*, 5 (3), 173-196.

Hensher, D.A. (2008) Climate change, enhanced greenhouse gas emissions and passenger transport - What can we do to make a difference?. *Transportation Research Part D*, 13 (2), 95-111.

Ho, H.W., Wong, S.C. (2005) Combined model of housing location and traffic equilibrium problems in a continuous transportation system. *Proceedings of the 16th International Symposium on Transportation and Traffic Theory* (ISTTT16), Maryland, U.S.A., July 19-21.

Ho, H.W., Wong, S.C. (2007) Housing allocation problem in a continuum transportation system, *Transportmetrica*, 3 (1), 21-39.

IEA (2006) *CO2 Emissions from Fuel Combustion 1971-2004*, Paris: International Energy Agency.

Joumard, R., Jost, P., Hickman, J., Hassel, D. (1995) Hot passenger car emissions modelling as a function of instantaneous speed and acceleration, *Science of The Total Environment*, 169, 167-174.

Lam, T., Niemeier, D. (2005) An exploratory study of the impact of common land-use policies on air quality, *Transportation Research Part D*, 10 (5), 365-383.

McNally, M.G., Kulkarni, A. (1997) Assessment of influence of land use-transportation system on travel behavior, *Transportation Resarch Record*, 1607, 105-115.

Messenger, T., Ewing, R. (1996) Transit-oriented development in the Sun Belt, *Transportation Resarch Record*, 1552, 145-153.

Nagurney, A. (2000a) Congested urban transportation networks and emission paradoxes, *Transportation Research Part D*, 5 (2), 145-151.

Nagurney, A. (2000b) Alternative pollution permit systems for transportation networks based on origin/destination pairs and paths, *Transportation Research Part D*, 5 (1), 37-58.

Nagurney, A., Qiang, Q., Naguney, L.S. (2010) Environmental impact assessment of transportation networks with degradable links in an era of climate change, *International Journal of Sustainable Transportation*, 4 (3), 154-171.

Nagurney, A., Ramanujam, P. (1998) A multimodal traffic network equilibrium model with emission pollution permits: Compliance vs noncompliance, *Transportation Research Part D*, 3 (5), 349-374.

Nowlan, D.M., Stewart, G. (1991) Downtown population growth and commuting trips: Recent experience in Toronto, *Journal of the American Planning Association*, 57 (2), 165-182.

Poudenx, P. (2008) The effect of transportation policies on energy consumption and greenhouse gas emission from urban passenger transportation. *Transportation Research Part A*, 42 (6), 901-909.

Rakha, H., Ahn, K., Trani, A. (2004) Development of VT-Micro model for estimating hot stabilized light duty vehicle and truck emissions. *Transportation Research Part D*, 9 (1), 49-74.

Scora, G., Barth, M. (2006) *Comprehensive Modal Emissions Model (CMEM), Version 3.01 User's Guide*. University of California, Riverside Center for Environmental Research and Technology.

WBCSD (2004) *Mobility 2030: Meeting the Challenges to Sustainability*. World Business Council for Sustainable Development

Wong, S.C. (1998) Multi-commodity traffic assignment by continuum approximation of network flow with variable demand. *Transportation Research Part B*, 32 (8), 567-581.

Wong, S.C., Lee, C.K., Tong, C.O. (1998) Finite element solution for the continuum traffic equilibrium problems. *International Journal for Numerical Methods in Engineering*, 43 (7), 1253-1273.

Yang, C., Mccollum, D., Mccarthy, R., Leighty, W. (2009) Meeting an 80% reduction in greenhouse gas emissions from transportation by 2050: A case study in California. *Transportation Research Part D*, 14 (3), 147-156.

Yin, Y., Lawphongpanich, S. (2006) Internalizing emission externality on road networks. *Transportation Research Part D*, 11 (4), 292-301.